2010-12-01

Comparison of H-alpha and H-beta Temperature Indices in the Hyades and Coma Star Clusters and Selected H-beta Standard Stars

Miriam Anne West
Brigham Young University - Provo

Comparison of Hα and Hβ Temperature Indices in the Hyades and Coma Star Clusters and Selected Hβ Standard Stars

Miriam Anne West

A thesis submitted to the faculty of
Brigham Young University
in partial fulfillment of the requirements for the degree of

Master of Science

Eric G. Hintz, Chair
Denise C. Stephens
Benjamin J. Taylor

Department of Physics and Astronomy

Brigham Young University

December 2010

ABSTRACT

Comparison of Hα and Hβ Temperature Indices in

the Hyades and Coma Star Clusters and

Selected Hβ Standard Stars

Miriam Anne West

Department of Physics and Astronomy

Master of Science

Using the Dominion Astrophysical Observatory's 1.2-m McKellar Telescope, we have obtained spectra on 81 stars from the Hyades Cluster, the Coma Cluster, and selected Hβ standard stars. These spectra cover from 4500 Å to 6900 Å which includes both the Hβ and Hα absorption lines. The Hβ absorption line has a long history of being used as a temperature index and more recently, calibration of an Hα index has been established for photometric observations. Through spectrophotometric comparison of temperature indices from the Hα and Hβ absorption lines we find the expected strong correlation between photometric indices based on the strength of these two lines. This result confirms that the Hα index is a strong indicator of temperature.

Keywords: color index, spectrophotometry, Hα index, Hβ index

ACKNOWLEDGMENTS

I would first of all like to thank my advisor Dr. Hintz for helping me get started with this project and for working with me along the way. I would also like to thank Professor Joner for lending his expertise in filter photometry and many other astronomy topics, Dr. Taylor for helping me with my statistical analysis, and Dr. Stephens for giving me many ideas on how to make my thesis better. I also want to thank Lisa Joner, Maureen Hintz, and Tabitha Bush for editing my drafts. I also thank Tabitha and Jeremy Schoonmaker for helping me learn spectra reduction methods in IRAF. I would most of all like to thank my husband Stephen and our little boy Brennen for their love and support as I've worked on this thesis.

Contents

List of Figures

Chapter 1

Introduction and Background

1.1 Project Motivation

We only observe a very tiny fraction of the light that a star emits, but astronomers have developed clever ways to glean considerable information from the light that we do receive. We can learn a lot about a star if we are able to measure its temperature. The temperature is a hard quantity to measure, however, because the temperature is not the only factor that contributes to the luminosity of the star. Stellar luminosity also depends on the radius of the star which is also challenging to measure.

Astronomers have developed several methods to estimate stellar effective temperature, but various methods have limitations, which will be discussed later in this chapter. The Hβ index was the first temperature index to be made where the index is based on a single absorption line. A temperature index based off of the Hα absorption line has also been created, but there is not a specific standard system developed on which to base these measurements. In the analysis for this project, we show that the Hα absorption line is a strong temperature indicator for stars with spectral types B-G. We also tested several different combinations of filters for both Hα and Hβ indices to see which filter combination shows the most sensitivity

to temperature.

1.2 Absorption Lines

Kirchoff's laws, as described in (Carroll & Ostlie, 1996), can help us understand the light that a star emits. If a dense gas is hot enough, it will radiate in the visible part of the spectrum. The spectrum will appear to be continuous, showing all colors. If a cooler gas cloud is placed in front of a dense hot gas, the cloud will absorb some of the photons and there will be dark lines in the continuous spectrum. The core of a star resembles a dense hot gas and its atmosphere resembles a cooler diffuse gas. Since the light produced in the core of the star has to pass through its atmosphere before we can detect it, light at certain wavelengths is absorbed and we observe dark absorption lines in the spectrum.

In order to understand how absorption lines are formed, we can look at the Bohr model of the atom. In the Bohr model, electrons orbit around the nucleus in discrete orbits and every orbit has an energy associated with it. If a photon with just the right amount of energy hits an atom, the photon will be absorbed and an electron will jump to a higher energy level. In order to get the electron to jump from one energy level to another, the energy of the photon has to be exactly equal to the difference in energy between the two levels. We can find the wavelength of the photon that was absorbed by using the equation λ=hc/E, where λ is the wavelength of the photon, h is Planck's constant, c is the speed of light, and E is the energy of the photon. Since the energy levels in an atom are quantized, every atom has distinct absorption lines that it can produce. We can then use the absorption lines to identify chemical species in the star.

Absorption lines produced in stars are well studied and are used to give a star its spectral classification. Since hydrogen is the most abundant element in stars, it makes sense that we would be able to see strong, or dark, hydrogen absorption lines. The first spectral

classification system was based on the strength of hydrogen lines. Stars with the strongest hydrogen lines were designated as A stars. The stars with the next strongest hydrogen lines were B stars, and so on. In today's system we still use the same letter designations, but the stars are ordered in terms of temperature instead. The stellar spectral types in order of hottest to coolest are OBAFGKM. To get a more specific spectral type, numbers 0-9 are assigned to each spectral type with 0 being the hottest and 9 being the coolest. For example, a G4 star would be hotter than a G8 star. In the optical part of the spectrum, the stars with the strongest hydrogen lines are the B, A, F, and G stars. The K and M stars are too cool to produce strong hydrogen lines and the O and the hottest B stars are so hot that they ionize much of the hydrogen in the atmosphere of the star.

The hydrogen spectral lines that appear in the visible part of the spectrum are called Balmer lines and occur when the electrons transition between the n=2 energy level and a higher energy level. The spectral line that results from the transition between the n=2 and the n=3 energy levels is the hydrogen alpha (Hα) line and is observed at a wavelength of 6563 Å. The line that results from the transition between the n=2 and n=4 energy levels is the hydrogen beta (Hβ) line and is found at 4861 Å. These wavelengths can easily be calculated, with the equation

$$\frac{1}{\lambda_{ab}} = R\left(\frac{1}{n_b^2} - \frac{1}{n_a^2}\right) \tag{1.1}$$

where R is the Rydberg constant which equals $1.097 * 10^7\ m^-1$ and n_b and n_a are the two different energy levels. Figure 1.1 shows the spectra for stars of different spectral type. The bottom axis labels the wavelength of the spectra and the left axis labels the spectral type. The top axis identifies the location of the Hα and Hβ lines. We can see in this figure that there are dark Hα and Hβ absorption lines in the B, A, F, and G stars. We can also see that the hydrogen absorption lines are faint in the O, K, and M stars.

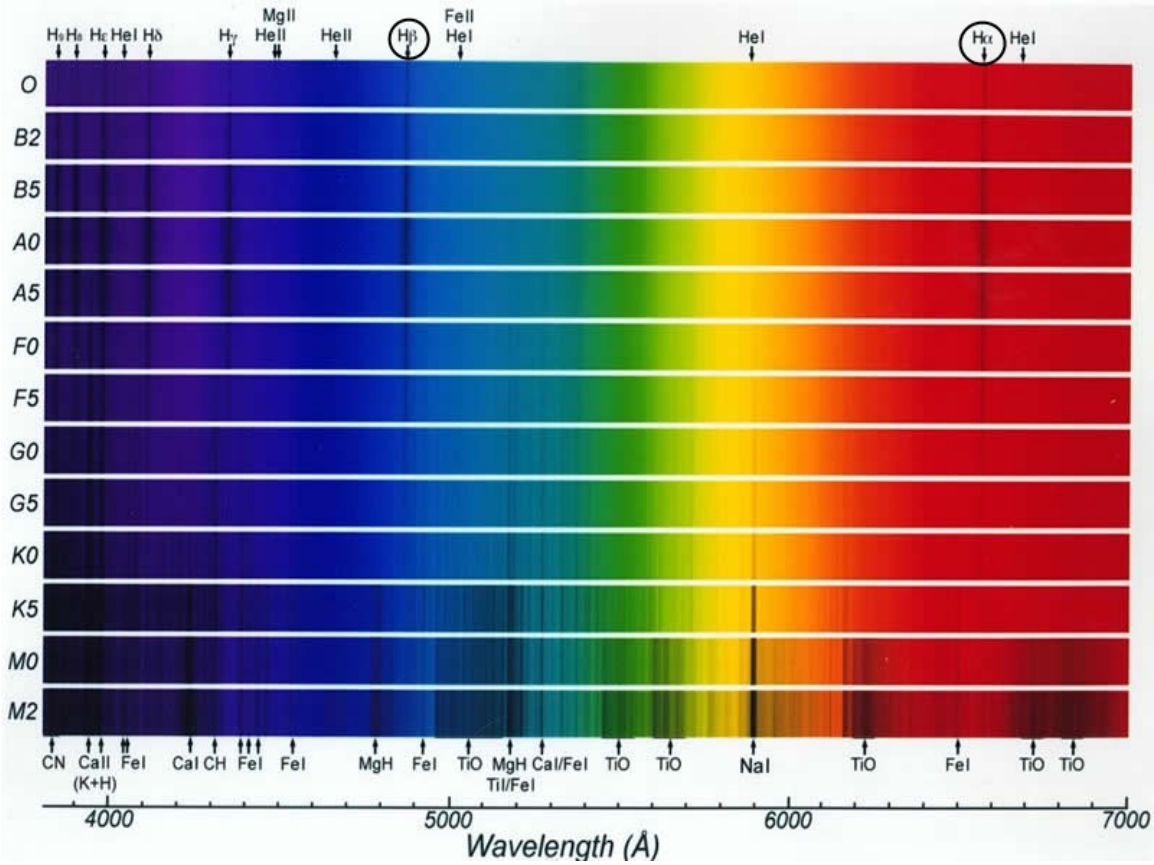

Figure 1.1 Spectra for stars of various spectral types. Image courtesy of academics.smcvt.edu

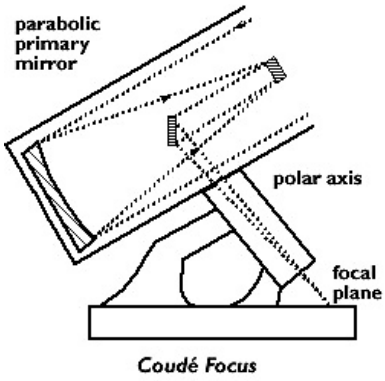

Figure 1.2 Coudé focus telescope diagram. Image courtesy of www.as.utexas.edu/astronomy/

1.3 Spectroscopy

The spectra for this project were secured using the DAO 1.2-m McKellar Telescope which has a Coudé focus. A diagram for a Coudé focus telescope is shown in Figure 1.2. The incoming light is reflected by the primary mirror to the secondary mirror. It is then reflected off a flat mirror, which directs the light down the polar axis of the telescope to the spectrograph.

In order to obtain the spectrum of a star, the light has to be dispersed into its component wavelengths. We can do this by using a spectrograph. First, the light passes through a diffraction grating, which spreads the light out into its component wavelengths. Then the spectrum is recorded on a CCD. A CCD is a charge coupled device that counts the number of photons that hit it. When photons hit the CCD, an electric charge will build up inside each pixel that is linearly related to the number of photons that hit it. The number of electrons is counted and used to digitally show the intensity of the incoming light. To study the light from the star, we plot the intensity of the light as a function of wavelength. An example of a calibrated spectrum from DAO can be seen in Figure 1.3. The x axis shows the wavelength of the light and the y axis shows relative intensity. The location of the Hα and Hβ absorption lines are also labeled on this graph.

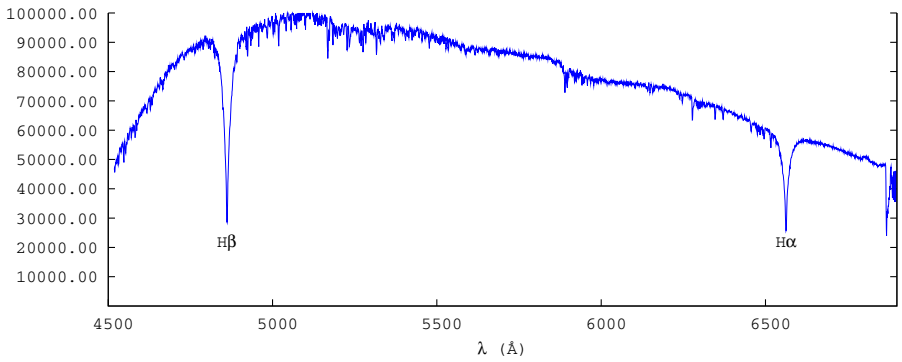

Figure 1.3 Spectrum of the star HR 63

1.4 Stellar Temperature

We can get a general idea for how hot a star is by looking at its color. Cooler stars are redder and hotter stars are bluer. Since a star's output resembles the output of a blackbody, we can use Wein's law to approximate the wavelength of its peak output. Wein's law can be written as

$$\lambda_{max} = \frac{2.898 * 10^7}{T} \tag{1.2}$$

where T is in Kelvin and λ_{max} is in angstroms. The wavelength at which the star radiates the most light is directly related to the blackbody temperature of the star.

Another way to find the temperature of a star is to measure the relative strengths of the absorption lines. The strength of the absorption line gives us an idea of the number of atoms undergoing the transitions necessary to produce that line. The Saha equation gives us the ratio of the number densities of atoms in different ionization states and can be expressed by the following equation:

$$\frac{n_{i+1}n_e}{n_i} = \frac{2}{\Lambda^3}\frac{g_{i+1}}{g_i}exp\left(\frac{-(\epsilon_{i+1} - \epsilon_i)}{kT}\right) \tag{1.3}$$

where n_i is the density of atoms in the ith state of ionization, n_e is the electron density, g_i is

the degeneracy states for the ions, ϵ_i is the energy required to remove an electron from ground state of the atom, E is the energy of the electron in each level, k is Boltzmann's constant, and T is temperature. Λ is the thermal de Broglie wavelength of an electron, which also depends on temperature. The Boltzmann equation gives us the ratio of the number densities of particles in different excited states and is written as

$$\frac{N_b}{N_a} = \frac{g_b}{g_a} \exp\left(\frac{-(E_b - E_a)}{kT}\right) \tag{1.4}$$

where N is the number density of particles in each state, g is the probability of the particles being in each state, k is Boltzmann's constant, and T is temperature. Both the Boltzmann and the Saha equations, as presented in (Carroll & Ostlie, 1996), depend on temperature and therefore the ratios of the strengths of different spectral features vary as functions of temperature.

1.5 Dual Wavelength Color Indices

As we saw in the previous section, the temperature of a star is related to its color, but we need a way to quantify color. Several dual wavelength color indices have been created to measure the color index of a star. The color index is defined to be the difference between a star's photometric magnitudes measured over two different wavelength regions. The long wavelength magnitude is subtracted from the short wavelength magnitude. Several dual wavelength indices have been developed, such as (b-y) in the Strömgren system. This system is calibrated so a star with a temperature of 10,000K will have a (b-y) value of 0.0. A star with a negative (b-y) value will be hotter than 10,000 K, and a star with a positive (b-y) value will be cooler than 10,000 K.

1.6 Single Wavelength Color Indices

Both dual wavelength and single wavelength color indices use measurements from two filters, but for single wavelength color indices both filters are centered on the same wavelength. One of the filters has a narrow passband and one has a wide passband. The narrow filter measures the amount of light from the absorption line and the wide filter measures the surrounding continuum. The flux from each filter is calculated and then converted into magnitude. The magnitude of the wide filter is subtracted from the magnitude of the narrow filter to get the color index. It can also be calculated directly from the flux measurements using the equation

$$\text{color index} = -2.5log\left(\frac{Flux(narrow)}{Flux(wide)}\right). \tag{1.5}$$

The final color index is reported in magnitudes. The larger the value of the index, the stronger the spectral line is.

1.7 Hα vs Hβ

The original single wavelength index system was developed by Crawford in 1966 and was based on the Hβ absorption line. The Hβ index is the most commonly used single wavelength color index, but there are reasons to suggest that an index based on the Hα line would be better.

The Hβ index was developed when the most commonly used detector was the photomultiplier. Some photomultipliers peak in quantum efficiency in the blue part of the spectrum, which is where the Hβ line is located. Now that CCDs are most commonly used to image stars, we are able to do better imaging in the red part of the spectrum which is where the Hα line is located.

1.8 Advantages of a Single Wavelength Index Over a Dual Wavelength Index

Before the light from a star reaches the Earth it travels through interstellar dust. Dust scatters the light from the star but does not scatter every wavelength evenly. Blue light gets scattered more than red light, so the light that we observe appears reddened. Single wavelength indices are reddening free because both filters are centered on the same wavelength and are therefore affected equally by interstellar reddening. Dual wavelength color indices measure the light from a star at two different wavelengths. If the light is reddened more in one filter than in the other, then we will not measure a correct color index. To get a correct index, the extinction must be corrected for or it may be necessary to base the index off of three colors rather than just two, which is generally more time consuming (Zeilik & Gregory, 1998).

It is also advantageous to use single wavelength color indices because they are not affected by atmospheric extinction. Similar to interstellar reddening, atmospheric extinction is wavelength dependent and affects the values of dual wavelength indices. Single wavelength indices remain unaffected, however, since the atmospheric extinction is identical for both filters since they have the same central wavelength.

Chapter 2

Observations

2.1 Spectroscopic Observations

Spectroscopic observations were made at the Dominion Astrophysical Observatory (DAO) over 10 observing runs from 2005 to 2008. The observations were secured using the 1.2-m McKellar Telescope and covered a wide spectral range from 4500 Å to 6900 Å which included both the Hα and Hβ spectral lines. The spectrograph was mounted at the Coudé focus. We used the 3231 grating which has 300 grooves/mm, is blazed at 4200 Å, and yields a dispersion of 41 Å/mm. The SITe4 camera was used, which has 15 micron pixels and yeilded a resolution of 0.615 Å/pixel.

Observations were taken of stars in the Hyades and Coma star clusters and a selection of Hβ standards from (Crawford & Mander, 1966) and (Taylor & Joner, 1992). These star clusters were observed because they are relatively close and many of their stars have well established Hβ values. The stars ranged in spectral types from O9 to M4.5, but most stars observed were spectral types B through G. Exposure times ranged from 100 to 1000 seconds. Table 2.1 lists the stars observed, number of observations, V magnitude, spectral type, effective temperature, Fe/H, and b-y, and the Hβ and Hα index values. Values for

V magnitude, Spectral Type, Fe/H, b-y were found using the (SIMBAD Database, 2010). Sources for temperature values can be found in Appendix A. Most Hβ values were found using (Crawford & Mander, 1966) and (Taylor & Joner, 1992). A few other Hβ values were found in (Crawford et al., 1966), (Crawford & Perry, 1966), (Crawford et al., 1972), and (Hauck & Mermilliod, 1980). Hα values were found in (Adams, 2009) and (Laverty, 2006).

Table 2.1. Previously published data

Star name	HD number	# Obs.	V mag	Spectral Type	T*eff* (K)	Fe/H	(b-y)	Hβ	Hα
HR 63	HD 001280	32	4.619	A2 V	8960	0.14	0.026	2.883	
HR 68	HD 001404	36	4.52	A2 V			0.028	2.902	
HR 675	HD 004252	21	5.294	A2 V	9260	0.33	0.01	2.871	2.302
HR 269	HD 005448	15	3.867	G0 IV/V			0.068	2.863	
HR 458	HD 009826	3	4.09	F8 V	6140	0.12	0.346	2.629	
HR 493	HD 010476	21	5.2	K1 V	5201	-0.2	0.492	2.56	2.087
HR 801	HD 016908	18	7.43	K0				2.676	
Hz 27	HD 023157	3	10.43	A0			-0.001	2.779	2.241
HR 1144	HD 023324	15	8.47	K0				2.741	2.119
vB 6	HD 024357	14	5.946	F4 V	6876	-0.26	0.223	2.712	2.207
vB 10	HD 025825	3	7.811	G0	5922	0.12	0.374	2.608	2.13
vB 13	HD 026345	8	6.576	F6 V	6528	-0.01	0.276	2.675	
vB 19	HD 026784	6	7.08	F8 V	6230	0.17	0.332	2.634	2.159
vB 33	HD 027459	17	5.242	F0 V	7434		0.129	2.809	
vB 35	HD 027524	5	6.779	F5 V	6462	-0.46	0.285	2.661	2.182
vB 37	HD 027561	5	6.578	F5 V	6580	-0.11	0.272	2.67	2.199
vB 44	HD 027731	6	7.159	F5	6380	0.13	0.3	2.655	
vB 48	HD 027808	8	7.125	F8 V	6146	0.12	0.338	2.634	2.165
vB 47	HD 027819	14	4.804	A7 V	8025	0.17	0.081	2.857	
vB 53	HD 027901	5	5.965	F4 V	6747		0.243	2.696	2.196
vB 54	HD 027934	17	4.21	A7 IV-V	8208		0.069	2.864	
vB 55	HD 027946	5	5.275	A7 V	7315		0.149	2.783	
vB 56	HD 027962	14	4.311	A2 IV	9231	0.4	0.02	2.891	2.308
vB 74	HD 028355	11	5.014	A7 V	7683		0.115	2.828	2.291
vB 84	HD 028556	5	5.395	F0 V	7294		0.154	2.79	
vB 108	HD 029488	17	4.675	A5 Vn	7987		0.088	2.849	2.287
vB 129	HD 032301	11	4.626	A7 V	8038		0.079	2.847	2.187
HR 2585	HD 050973	12	10.91	M4.5				2.868	
HR 2880	HD 059881	9	5.245	F0 III	7636	0.19	0.128	2.790	
HR 3928	HD 086146	7	5.118	F6 Vs			0.298	2.652	2.174
HR 3951	HD 086728	9	5.4	G3 Va	5753	0.2	0.418	2.602	2.125

Table 2.1 (continued)

Star name	HD number	# Obs.	V mag	Spectral Type	T*eff* (K)	Fe/H	(b-y)	Hβ	Hα
HR 4456	HD 100600	9	5.95	B4 V			-0.067	2.681	2.19
HR 4540	HD 102870	7	3.61	F9 V	6100	0.12	0.354	2.628	
Tr 10	HD 105805	6	5.999	A4 Vn			0.069	2.859	2.295
Tr 62	HD 107168	5	6.239	A8 m	8129	0.35	0.079	2.876	2.309
Tr 90	HD 107685	3	8.54	F6	6380	-0.09	0.304	2.645	2.16
Tr 130	HD 108382	12	4.965	A4 V			0.053	2.87	2.304
Tr 144	HD 108642	3	6.54	A2 m			0.098	2.842	2.287
Tr 145	HD 108651	3	6.65	A0 p	7875	0.39	0.012	2.841	2.296
Tr 162	HD 108976	3	8.54	F6 V	6345	-0.04	0.307	2.644	2.156
Tr 183	HD 109307	3	6.265	A4 Vm	8400	0.16	0.056	2.884	2.32
HR 4931	HD 113139	6	4.93	F2 V			0.244	2.708	
HR 5011	HD 115383	3	5.22	G0 Vs	5866	0.1	0.373	2.617	2.142
HR 5270	HD 122563	6	6.2	F8 IV	4500	-2.75	0.631	2.525	2.093
HR 5447	HD 128167	6	4.46	F2 V	6700	-0.38	0.253	2.681	
HR 5511	HD 130109	6	3.72	A0 V			0.005	2.846	
	HD 140283	3	7.212	F3	5650	-2.3	0.379	2.575	2.12
HR 5933	HD 142860	6	3.85	F6 IV	6254	-0.18	0.319	2.633	
HR 5936	HD 142908	21	5.44	F0 IV	6908	-0.02	0.233	2.707	2.205
HR 5968	HD 143761	15	5.4	G0 Va	5782	-0.24	0.393	2.59	2.123
HR 6355	HD 154494	6	4.882	A4 IV			0.063	2.878	
	HD 161817	6	6.988	A2 V	7636	-1.3	0.126	2.764	2.226
HR 6629	HD 161868	6	3.75	A0 V			0.023	2.908	
HR 6852	HD 168270	6	6.236	B9 V			0.032	2.811	
HR 6977	HD 171623	6	5.792	A0 Vn			0.022	2.819	
HR 7069	HD 173880	27	4.346	A5 III	8542	-0.19	0.055	2.898	
HR 7178	HD 176437	30	3.24	B9 III	10080	0.11	0.003	2.727	
HR 7235	HD 177724	21	2.988	A0 Vn			0.012	2.842	2.24
HR 7253	HD 178233	33	5.529	F0 III			0.176	2.759	
HR 7446	HD 184915	6	4.963	B0.5 III			0.084	2.565	
HR 7447	HD 184930	6	4.349	B5 III			-0.015	2.711	
HR 7462	HD 185144	24	4.7	K0 V	5298	-0.21	0.472	2.568	

2.2 Image Processing

Images were reduced using standard spectral reduction packages in the Image Reduction and Analysis Facility (IRAF). The process of reducing data transforms raw data into a form where calibrated measurements can be made. For this analysis the images were processed using the following steps.

2.2.1 Updating Headers

Every image file has a corresponding header file. This file contains information about the telescope and the observation. Some examples of information needed in the header files are the object name, the image type, the date and time of the observation and so on. This information is used by IRAF to correctly perform operations on the data. Generally headers are not complete and information needs to be added to them. The task *hedit* can add information into the header and the task *asthedit* uses a .cmds file to add a batch of information. Once the headers have been updated, other information can be calculated. The command *setjd* calculates the Julian date of the day the observation was taken. The command *setairmass* is performed on all object frames, which calculates the amount of the Earth's atmosphere that the telescope is pointing through to view an object. All processing done on a data frame is recorded in the header file.

2.2.2 Trimming Frames

When observations are recorded on a CCD, sometimes the edges of the image do not contain any information. Figure 2.1 shows an unprocessed spectra. The x axis shows the uncalibrated wavelength dispersion and the y axis shows relative intensity. In this image we can see that there is no signal for most of the columns past the value 4000 on the x axis. These columns can be removed using the *ccdproc* command. We removed columns 1-25 and 4001-4200 from

Table 2.1 (continued)

Star name	HD number	# Obs.	V mag	Spectral Type	T*eff* (K)	Fe/H	(b-y)	Hβ	Hα
HR 7469	HD 185395	30	4.48	F4 V	6700	0.01	0.261	2.681	2.221
HR 7503	HD 186408	18	5.96	G1.5 V	5800	0.06	0.409	2.602	2.133
HR 7504	HD 186427	21	6.2	G3 V	5760	0.06	0.416	2.596	2.132
HR 7534	HD 187013	27	4.99	F7 V	6289	-0.09	0.311	2.649	2.176
HR 7560	HD 187691	23	5.1	F8 V	6090	0.07	0.356	2.63	2.148
HR 7610	HD 188728	17	5.29	A1 IV	9509	0.47	-0.005	2.902	2.324
HR 7730	HD 192514	12	4.833	A5 III			0.068	2.802	
HR 7906	HD 196867	6	3.771	B9 IV				2.802	
HR 7977	HD 198478	9	4.858	B3 Iae	14900	-0.23	0.356	2.53	
HR 8143	HD 202850	14	4.342	B9 Iab			0.139	2.584	
HR 8279	HD 206165	6	4.788	B2 Ib	17760	-0.33	0.277	2.56	
HR 8494	HD 211336	15	4.19	F0 IV			0.171	2.757	
HR 8585	HD 213558	9	3.777	A1 V			0.002	2.908	
HR 8622	HD 214680	9	4.877	O9 V			-0.067	2.587	
HR 8826	HD 218918	9	5.157	A5 Vn			0.164	2.821	
HR 8965	HD 222173	9	4.3	B8 V			-0.031	2.728	
HR 8969	HD 222368	9	4.13	F7 V	6170	-0.15	0.33	2.622	
HR 8976	HD 222439	24	4.137	B9 IV			-0.035	2.834	
HR 9088	HD 224930	30	5.75	G5 Vb	5413	-0.81	0.428	2.567	2.106

Note. — Values for V magnitude, Spectral Type, Fe/H, b-y were found using the (SIMBAD Database, 2010). Sources for temperature values can be found in Appendix A. Hβ values were found in (Crawford & Mander, 1966), (Crawford et al., 1966), (Crawford & Perry, 1966), (Crawford et al., 1972), (Hauck & Mermilliod, 1980), and (Taylor & Joner, 1992). Hα values were found in (Adams, 2009) and (Laverty, 2006).

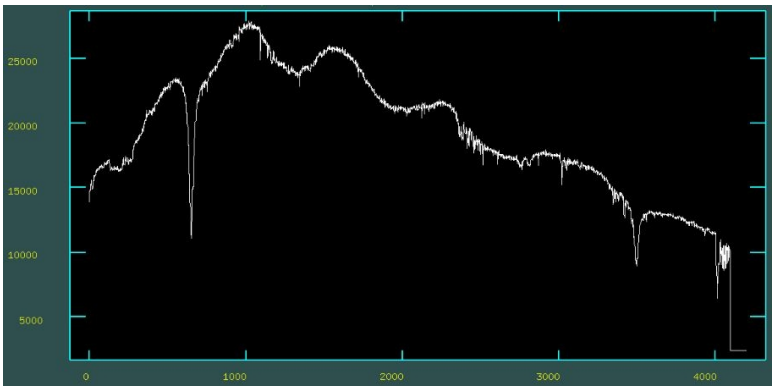

Figure 2.1 Unprocessed Spectra of a Star

Figure 2.2 Bias Frame CCD Image.

our images for this investigation.

2.2.3 Processing Bias Frames

Bias frames, also called zero frames, are taken to measure the residual electrons from CCD readout electronics. The images are taken for zero seconds with the camera shutter closed. An image of a bias frame is shown in Figure 2.2. Typically about 30 bias frames were taken with each night of data. The bias frames are combined using the command *zerocombine* to make an averaged bias frame. The combined image is then subtracted from the other calibration frames and the object frames.

2.2.4 Processing Flat Frames

Flat frames are taken because pixels across the CCD do not all respond equally to light. We took camera flats to correct for this. A camera flat frame is taken by exposing the CCD to

Figure 2.3 Flat Frame CCD image.

an even amount of light from a flood lamp with a light diffuser placed in front of the lamp. About 25 flat frames were taken during each night of observation. The command *flatcombine* is then used to get an average flat image. Most of the signal from the flat is recorded in the center of the CCD as shown in Figure 2.3. Using the task *apflatten*, we can define an aperture so we only use the part of the CCD that contains the most signal. The final result is applied to all object frames using *ccdproc*.

2.2.5 Removing Cosmic Rays

The task *cosmicrays* can be used to remove cosmic ray hits from images of spectra. The default settings were adequate in removing most cosmic ray hits, but a few of the larger cosmic ray hits had to be removed by hand.

2.2.6 Wavelength Calibration

When we record the image of the spectrum of a star, we record the intensity of the light versus wavelength. The true wavelengths of the spectral features are not recorded, however, so we use comparison frames called arcs to calibrate them. Arcs are images taken of the spectra from Iron/Argon or Thorium/Argon arc lamps. The arc lamps have prominent emission lines from the different elements and we can identify them and match them up to each stellar spectrum. Generally an arc frame is taken before and after every object frame so the orientation of the telescope is the same for both object and comparison frames. The task in IRAF that we use to apply the wavelength calibration is called *doslit*. Also in *doslit*, we define an aperture for each star to select the part of the star with the most signal. Figure

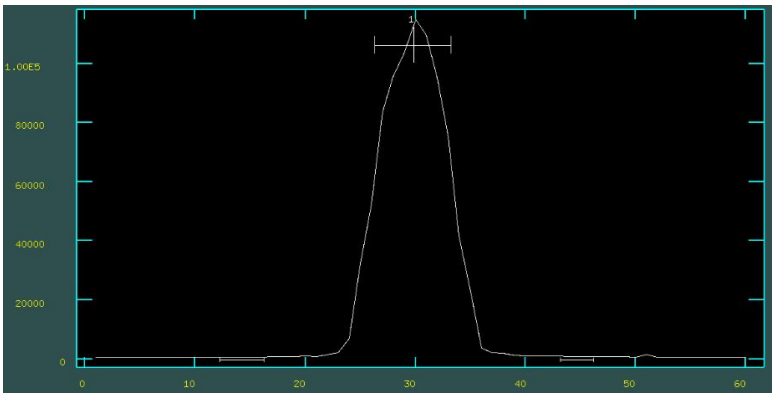

Figure 2.4 Aperture of a star

2.4 shows the image of an aperture. The x axis shows the 60 pixel cross section of the CCD chip and the y axis shows the relative intensity of the star. That aperture is then compressed by averaging over the aperture so the final image we are taking measurements off of is one dimensional rather than two dimensional.

2.3 Spectrophotometry

After an object frame has been wavelength calibrated in *doslit*, the color index can be measured from it. We used the IRAF task *sbands* to calculate the Hα and Hβ indices. *Sbands* takes a user defined filter function and measures the magnitude that would be found if a star were photometrically observed through that filter. In order to run *sbands* we need three different types of text files. The first is a list of input spectra. This is simply a list of spectra image files that the user wishes to take measurements from. Second, we need a bandpass file. The bandpass file contains the filter identification name, the central wavelength of the bandpass, the width of the bandpass, and the name of the filter function text file, which is the third text file needed. If there is no filter function specified, *sbands* will assume a square filter with a transmission of 100% across the entire width of the filter.

The filter function text file has two columns. The first is a list of wavelengths covered by the filter, and the second is the filter response at each wavelength. The user can either input a set of wavelength responses that match the transmission curve of a real filter or the user can create a theoretical filter function.

In order to take a spectrophotometric measurement of the single wavelength index, the user must input both a wide filter function and a narrow filter function. *Sbands* will calculate the resulting flux from each filter by using the equation

$$flux = \Sigma(pix_n * response_n) \tag{2.1}$$

where pix_n is each pixel in the bandpass and $response_n$ is filter response at that pixel. The magnitude of each filter is calculated with the equation

$$magnitude = -2.5log(flux). \tag{2.2}$$

The final index value is found when the magnitude from the wide filter is subtracted from the magnitude of the narrow filter.

2.3.1 Filter Functions

The shapes of the Hα and Hβ transmission curves that we used to make all of the spectrophotometric measurements can be seen in Figure 2.5. The Hα narrow filter has a FWHM of 30 Å, and the Hα wide filter has a FWHM of 210 Å. The FWHM of the Hβ narrow filter is 28 Å and the FWHM of the Hβ filter is 130 Å. These transmission curves are based off of traces of actual filters that were created using a scanning spectrophotometer. The Hα traces were made from the filters used by (Adams, 2009) and (Laverty, 2006). The Hβ traces were made from filters that approximate the filters used by (Crawford & Mander, 1966). The narrow filter from their paper has a FWHM of about 30 Å, and the wide filter has a FWHM of about 150 Å.

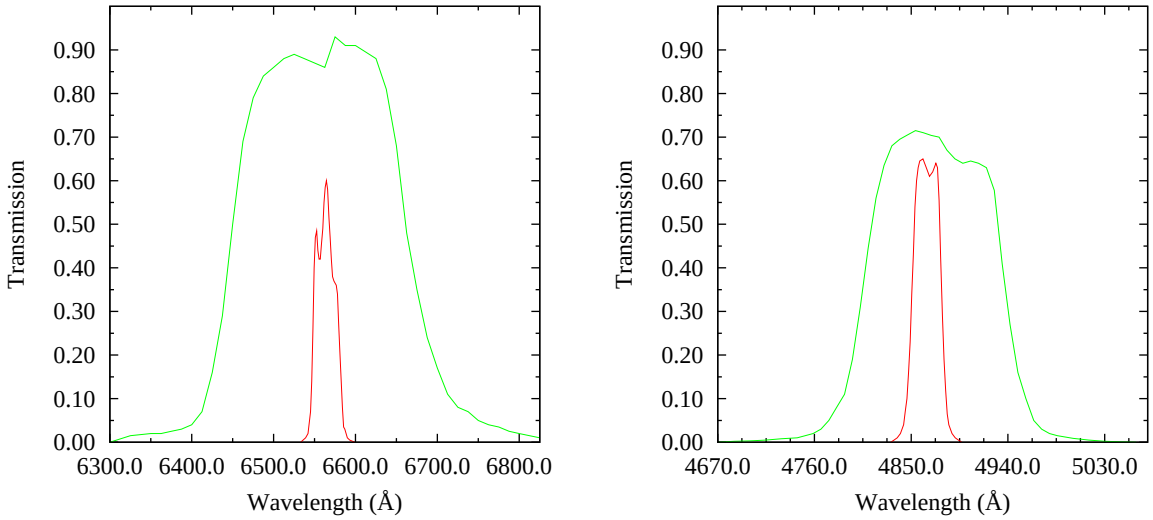

Figure 2.5 Left: Hα filters, Right: Hβ filters

Figure 2.6 shows an Hα absorption line plotted with a simulated narrow transmission gaussian curve having a FWHM of 20 Å and a simulated wide transmission curve of 200 Å. This figure shows how much of the absorption line is being measured through each filter. The narrow filter measures the core of the absorption line and the wide filter measures the entire absorption line and the surrounding continuum.

In addition to the filter functions that we created to match existing filters, we also created several theoretical filters. Table 2.2 displays all of the filter functions created for this project. All synthetic filters have a maximum transmission of 100%. Each filter has a gausian shape and was created using the equation

$$f(x) = a \exp\left(\frac{-(x-b)^2}{2c^2}\right) \tag{2.3}$$

where c=FWHM/$(2\sqrt{2ln(2)})$. We created these filter functions so we could test combinations of narrow and wide filters to see which combination shows the greatest sensitivity to temperature. From these measurements, we can determine if we should make index measurements with common filters or if it is necessary to design a new filters with specific widths.

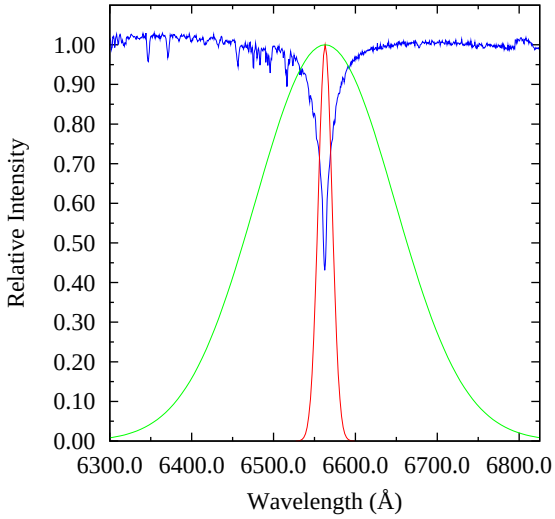

Figure 2.6 Narrow and wide simulated filters centered on the Hα absorption line

Table 2.2. Model Filter Functions

Filter Identification	Filter Shape	FWHM	Center Wavelength	Total Width
αnarrow20g	gaussian	20	6563	64
αnarrow30g	gaussian	30	6563	80
αwide100g	gaussian	100	6563	320
αwide125g	gaussian	125	6563	400
αwide150g	gaussian	150	6563	480
αwide175g	gaussian	175	6563	560
αwide200g	gaussian	200	6563	600
βwide100g	gaussian	100	4861	320
βwide125g	gaussian	125	4861	400
βwide150g	gaussian	150	4861	480
βwide175g	gaussian	175	4861	560
βwide200g	gaussian	200	4861	590

Chapter 3

Analysis and Results

3.1 Transforming Instrumental Indices to Standard Values

Each night of data had to be converted from instrumental indices to standard indices. Standard Hβ values for this set of stars were found in (Crawford & Mander, 1966), (Taylor & Joner, 1992), (Crawford et al., 1966), (Crawford et al., 1972), (Hauck & Mermilliod, 1980), and (Crawford & Perry, 1966). Standard Hα values were found in (Adams, 2009) and (Laverty, 2006). We used the least squares method to compare the instrumental indices to the standard indices. From this method we found a linear relationship between the instrumental indices and the standard indices. For each night of data, we found the slope and the zeropoint needed to transform the instrumental indices to standard indices. Then the instrumental indices were plugged into the linear equation

$$calibrated\ index = slope * (instrumental\ index) + zeropoint \tag{3.1}$$

to find the calibrated indices.

The process of transforming the instrumental Hβ indices to standard indices was very

straightforward because all of the stars in this data set had published Hβ indices. When transforming the Hα indices, however, the process was more complicated because there were not as many published Hα indices with which to compare the instrumental indices. We found that the best solution to this problem was to start with the night of data that had the largest number of stars with published Hα values. We used the least squares method on all of the stars that had a standard Hα index value. After the slope and zeropoint were determined, all instrumental index values were plugged into Equation 3.1. If there were any stars that did not have a published Hα index value, the newly calculated index value for each star was used as a standard value when transforming other nights of data. This iterative process was used until the data from each night was converted from instrumental indices to standard indices.

After the indices of our stars from each night of data were transformed to standard indices, the values for each star were averaged and the error of the mean was calculated. The error of the mean was calculated using Equation 3.2.

$$\sigma_m = \frac{\sigma}{\sqrt{N}} = \sqrt{\left(\frac{\Sigma(x_{mean} - x_i)^2}{N(N-1)}\right)} \tag{3.2}$$

All of the final standard indices and the corresponding error of the mean values can be found in Table 3.1. The average error values that we get for Hα is 0.0008 and the average error values that we get for Hβ is 0.0020. These error values are comparable to the error values obtained by (Crawford & Mander, 1966).

A graph of the Hα values versus the Hβ values can be found in Figure 3.1. The O and B stars are represented by the green circles, the outliers are represented by the purple circles, and the blue circles represent the rest of the stars. The line of best fit was also plotted and has an equation of Hα=0.633Hβ+0.487. The standard error for the slope is 0.009 and the standard error for the zeropoint is 0.024. This graph shows a very strong relation between the Hα and the Hβ indices and yields an R^2 value of 0.985. The two outliers were not used

in calculating the line of best fit because each outlier was more than $5\sigma_{rms}$ away from the line of best fit. The outlier on the left is HR 6977 and the outlier on the right is HR7977. HR6977 has some emission in the Hα absorption line so the Hα index value is smaller than expected. HR7977 is a B3 star which sometimes have weaker Hα absorption lines compared to the Hβ absorption lines.

Table 3.1. Measured Hα and Hβ values

Star name	Hα mag	Hα σ_m mag	# Obs.	Hβ mag	Hβ σ_m mag	# Obs.
HR 63	2.3062	0.0005	29	2.8782	0.0009	32
HR 68	2.3160	0.0005	30	2.8950	0.0017	36
HR 675	2.3040	0.0014	18	2.8782	0.0013	21
HR 269	2.2972	0.0008	9	2.8695	0.0017	15
HR 458	2.1440	0.0012	3	2.6234	0.0050	3
HR 493	2.0945	0.0011	15	2.5680	0.0015	21
HR 801	2.1784	0.0022	18	2.6721	0.0015	18
HD 23157	2.2442	0.0008	3	2.7729	0.0017	3
HR 1144	2.2203	0.0020	15	2.7413	0.0042	15
vB 6	2.2147	0.0007	11	2.7176	0.0009	14
vB 10	2.1390	0.0003	3	2.6140	0.0007	3
vB 13	2.1905	0.0002	8	2.6762	0.0020	8
vB 19	2.1603	0.0006	3	2.6390	0.0005	6
vB 33	2.2683	0.0005	17	2.8092	0.0034	17
vB 35	2.1859	0.0007	5	2.6743	0.0038	5
vB 37	2.1937	0.0022	5	2.6817	0.0056	5
vB 44	2.1784	0.0016	6	2.6673	0.0036	6
vB 47	2.2960	0.0005	14	2.8553	0.0009	14
vB 48	2.1613	0.0019	5	2.6385	0.0024	8
vB 53	2.2013	0.0010	5	2.7030	0.0042	5
vB 54	2.2988	0.0007	17	2.8654	0.0016	17
vB 55	2.2496	0.0009	5	2.7774	0.0088	5
vB 56	2.3126	0.0003	14	2.8959	0.0014	14
vB 74	2.2851	0.0006	11	2.8280	0.0052	11
vB 84	2.2565	0.0002	5	2.8013	0.0040	5
vB 108	2.2855	0.0004	17	2.8579	0.0024	17
vB 129	2.2900	0.0004	11	2.8558	0.0029	11
HR 2585	2.2974	0.0004	12	2.8695	0.0013	12
HR 2880	2.2451	0.0004	9	2.7900	0.0015	9
HR 3928	2.1742	0.0004	7	2.6537	0.0019	7
HR 3951	2.1269	0.0004	9	2.6001	0.0013	9

Table 3.1 (continued)

Star name	Hα mag	Hα σ_m mag	# Obs.	Hβ mag	Hβ σ_m mag	# Obs.
HR 4456	2.1785	0.0003	9	2.6677	0.0011	9
HR 4540	2.1535	0.0005	7	2.6243	0.0024	7
TR 10	2.2889	0.0006	6	2.8557	0.0027	6
TR 62	2.3077	0.0021	5	2.8764	0.0010	5
TR 90	2.1653	0.0050	3	2.6551	0.0065	3
TR 130	2.3042	0.0007	12	2.8705	0.0016	12
TR 144	2.2895	0.0002	3	2.8403	0.0011	3
TR 145	2.2981	0.0005	3	2.8340	0.0007	3
TR 162	2.1711	0.0005	3	2.6398	0.0043	3
TR 183	2.3158	0.0001	3	2.8848	0.0003	3
HR 4931	2.2112	0.0003	3	2.7042	0.0009	3
HR 5011	2.1448	0.0005	3	2.6302	0.0028	3
HR 5270	2.0774	0.0002	6	2.5329	0.0007	6
HR 5447	2.1971	0.0003	3	2.6650	0.0003	3
HR 5511	2.2817	0.0003	6	2.8428	0.0010	6
HD 140283	2.1165	0.0001	3	2.5699	0.0013	3
HR 5933	2.1629	0.0004	6	2.6320	0.0005	6
HR 5936	2.2077	0.0005	18	2.7077	0.0016	18
HR 5968	2.1298	0.0004	15	2.5956	0.0008	15
HR 6355	2.3072	0.0024	6	2.8782	0.0023	6
HD 161817	2.2024	0.0002	3	2.7328	0.0027	6
HR 6629	2.3175	0.0002	6	2.8937	0.0008	6
HR 6852	2.2599	0.0006	6	2.8071	0.0040	6
HR 6977	2.2175	0.0003	6	2.8130	0.0016	6
HR 7069	2.3167	0.0009	26	2.8836	0.0020	27
HR 7178	2.2310	0.0026	24	2.7358	0.0052	30
HR 7235	2.2928	0.0006	18	2.8652	0.0017	21
HR 7253	2.2347	0.0009	27	2.7557	0.0012	33
HR 7446	2.1018	0.0010	6	2.5670	0.0027	6
HR 7447	2.1984	0.0003	6	2.7092	0.0026	6
HR 7462	2.1021	0.0009	18	2.5601	0.0017	24

Table 3.1 (continued)

Star name	Hα mag	Hα σ_m mag	# Obs.	Hβ mag	Hβ σ_m mag	# Obs.
HR 7469	2.1938	0.0004	24	2.6824	0.0011	30
HR 7503	2.1266	0.0005	15	2.6015	0.0012	18
HR 7504	2.1266	0.0010	18	2.5952	0.0014	21
HR 7534	2.1699	0.0013	24	2.6473	0.0020	27
HR 7560	2.1540	0.0007	20	2.6284	0.0020	23
HR 7610	2.3210	0.0008	17	2.9051	0.0010	17
HR 7730	2.2514	0.0005	12	2.8011	0.0011	12
HR 7906	2.2649	0.0003	3	2.8030	0.0014	6
HR 7977	2.0331	0.0007	9	2.5296	0.0015	9
HR 8143	2.0837	0.0001	14	2.5767	0.0016	14
HR 8279	2.0786	0.0041	6	2.5515	0.0021	6
HR 8494	2.2342	0.0008	15	2.7563	0.0011	15
HR 8585	2.3173	0.0006	6	2.9067	0.0018	9
HR 8622	2.1416	0.0008	9	2.5854	0.0005	9
HR 8826	2.2647	0.0007	9	2.8212	0.0012	9
HR 8965	2.2138	0.0004	9	2.7218	0.0009	9
HR 8969	2.1597	0.0006	9	2.6299	0.0014	9
HR 8976	2.2795	0.0004	18	2.8283	0.0021	24
HR 9088	2.1095	0.0007	27	2.5667	0.0006	30

3.2 Comparison of the Hα and Hβ indices to the b-y color index and temperature

In order to compare how the Hα index compares to other color indices, we plotted it against the b-y color index in Figure 3.2. The top graph shows Hα vs. b-y and the bottom graph shows Hβ vs. b-y. The green circles represent stars in the Hyades cluster, the purple circles represent stars in the Coma cluster, the orange circles represent the outliers, and the blue circles represent the rest of the stars. We can see that both the Hα and the Hβ indices have

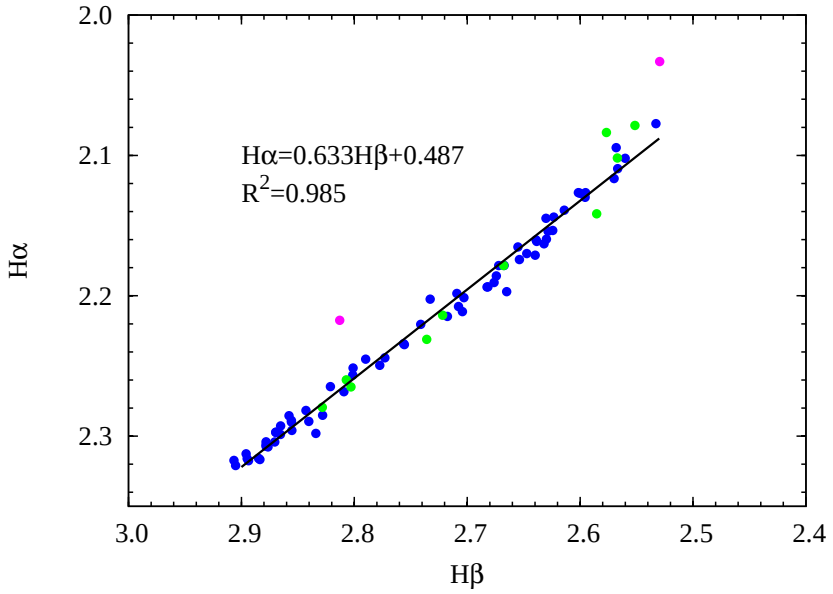

Figure 3.1 Hα vs. Hβ. The O and B stars are represented by the green circles, the outliers are represented by purple circles, and the blue circles represent the rest of the stars.

the strongest values at a b-y value of zero. There is a clear trend line for positive b-y values, but there is more scatter for negative b-y values for both the Hα and Hβ values. The scatter in the negative values for b-y occurs because some of the b-y values are reddened and the Hα and Hβ indices are reddening free. The outliers on this graph, represented by the orange circles, can also be explained by reddening. HR 7456, HR 7977, HR 8143, and HR 8279 are highly reddened B stars, which makes their b-y values shift to the right on this plot.

We plotted the Hα and Hβ indices against temperature in Figure 3.3 to see how strong of a correlation there is between the indices and temperature. The top graph shows Hα vs. Temperature and the bottom graph shows Hβ vs. Temperature. The green circles represent stars in the Hyades cluster, the purple circles represent stars in the Coma cluster, the orange and black circles represent the outliers, and the blue circles represent the rest of the stars. There is a strong relation for both the Hα and Hβ to temperature. As we expected, the

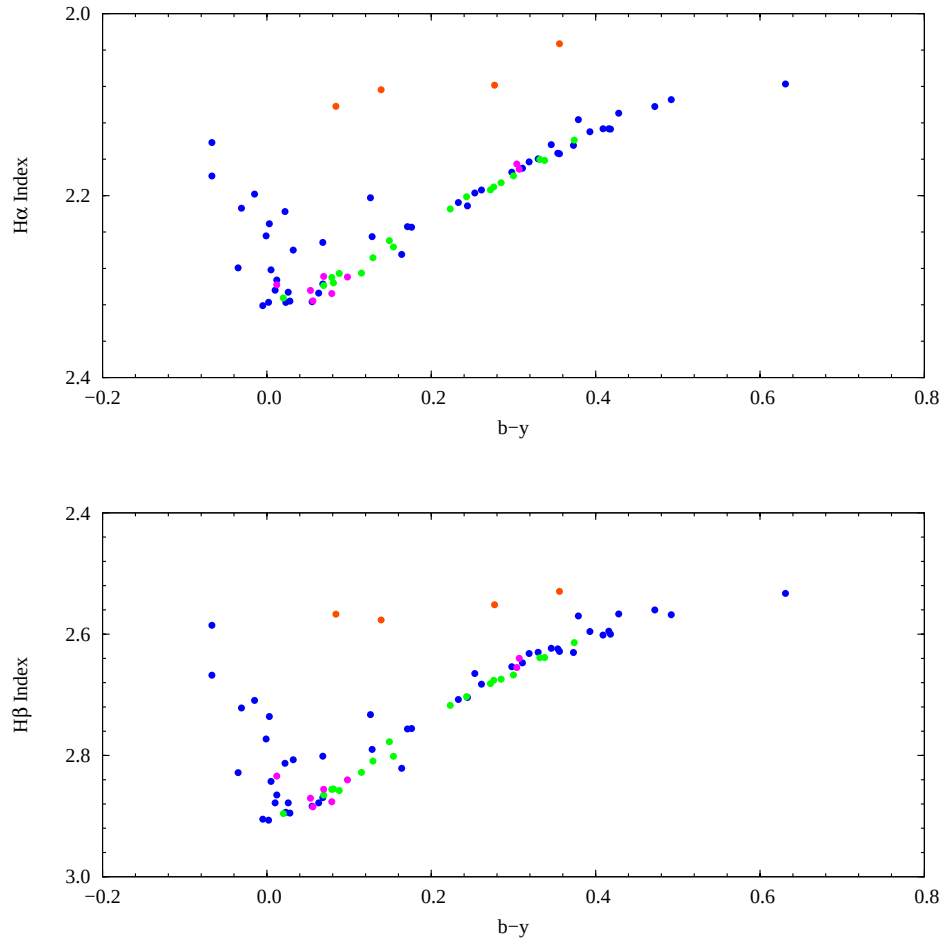

Figure 3.2 The top graph shows Hα vs. b-y and the bottom graph shows Hβ vs. b-y. The green circles represent stars in the Hyades cluster, the purple circles represent stars in the Coma cluster, the orange circles represent the outliers, and the blue circles represent the rest of the stars.

temperature sensitivity of both indices start to drop off at about 8,000 K because at higher temperatures, the hydrogen in the atmosphere of these hotter stars begins to ionize.

In Figure 3.4 we plotted Hα and Hβ vs. Temperature again but in this case we only plotted stars with temperatures between 5200 K and 8550 K. We removed the star represented by the black circle in figure 3.3 because it was more than $3\sigma_{rms}$ away from the line of best fit. Spectral types for these stars range from A through K. The Hα index values are shown on the top graph and the Hβ index values are shown on the bottom graph. We found relations for each index compared to temperature. The relation between the Hα index and temperature is Hα=7.20*10^{-5}T+1.72 with an R^2 value of 0.987. The relation between the Hβ index and temperature is Hβ=1.11*10^{-4}T+1.95 with an R^2 value of 0.98.

3.3 Filter Comparisons

By taking our Hα and Hβ index measurements spectrophotometrically, we have the advantage of being able to measure the Hα and Hβ indices through many different filter functions. We can make traces of filters that are currently used or we can create filter functions based off of any theoretical shape we want. This allows us to be able to test different narrow and wide filters and find which combination gives the best sensitivity.

We used *sbands* in IRAF to measure the Hα and Hβ indices from the data obtained on July 31, 2007. We chose this night of data because there were a large number of stars observed and they ranged in spectral type from O9 to K0. We tested 15 combinations of narrow and wide filters. We then plotted the instrumental indices for every filter combination against standard indices shown in Figures 3.5 through 3.7. The line of best fit for each filter combination was also plotted and the equations for each line were stated. The equations with the largest slope show the greatest sensitivity.

Figure 3.5 shows measurements centered on the Hα absorption line. The narrow filter

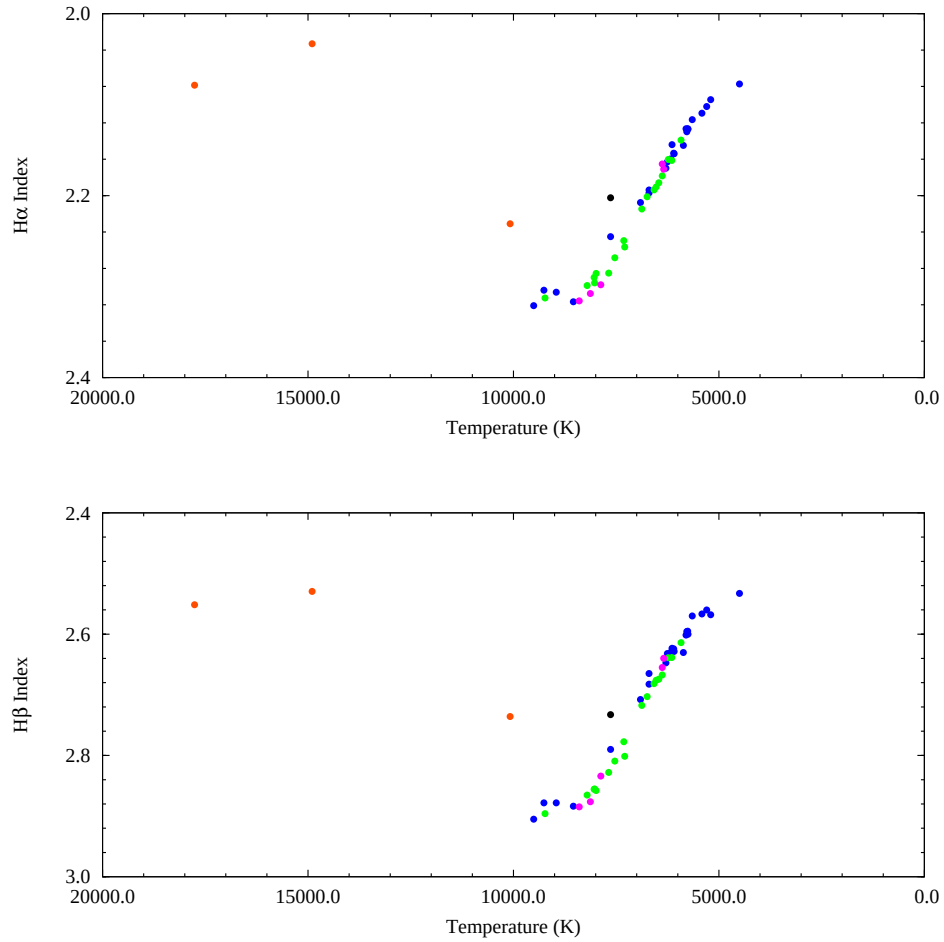

Figure 3.3 The top graph shows Hα vs. Temperature and the bottom graph shows Hβ vs. Temperature. The green circles represent stars in the Hyades cluster, the purple circles represent stars in the Coma cluster, the orange and black circles represent the outliers, and the blue circles represent the rest of the stars.

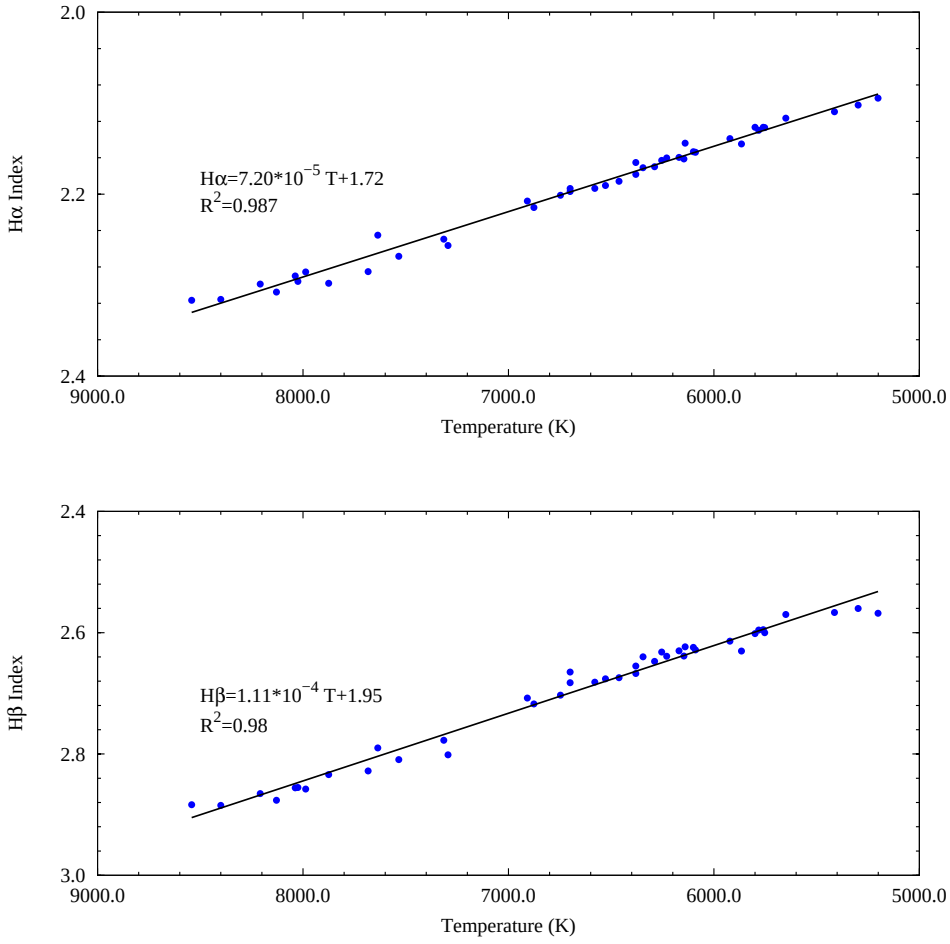

Figure 3.4 The top graph shows Hα vs. Temperature and the bottom graph shows Hβ vs. Temperature. The stars in this data set have spectral types A through K.

used in each of these measurements was filter αnarrow30g. This filter was used in combination with five different wide filters. The red circles correspond to measurements taken with the αwide100g filter. The green circles correspond to measurements taken with the αwide125g filter. The blue circles correspond to measurements taken with the αwide150g filter. The purple circles correspond to measurements taken with the αwide175g filter. The orange circles correspond to measurements taken with the αwide200g filter. All five sets of data had R^2 values greater than 0.99 and the slope for each data set has a standard error of less than 0.007. In this graph every line has a slope of less than unity, which means that none of these filter combinations has more sensitivity than the standard system.

Figure 3.6 shows measurements centered on the Hα absorption line. The measurements for this graph were taken with the same five wide filters as in Figure 3.5, but the narrow filter used was αnarrow20g. All five sets of data had R^2 values greater than 0.99 and the slope for each data set has a standard error of less than 0.011. In this graph, all of the lines have slopes greater than unity, which shows that every one of these filter combinations has more sensitivity than the standard system. This shows us that if we decrease the width of the narrow filter, we will increase our sensitivity. The combination that yielded the best sensitivity was the narrow filter αnarrow20g and the wide filter αwide200g with a slope of 1.29 compared to the standard system.

Figure 3.7 shows measurements centered on the Hβ absorption line. The measurements for this graph were taken with the same narrow filter used to measure the standard Hβ value. The graph of this transmission curve can be seen in Figure 2.5. As we can see in the graph of the Hβ filters, the narrow filter has a maximum transmission of only 65%. For the measurements in Figure 3.7 we scaled this narrow curve to a transmission of 100% in order to stay consistent with the wide filters which also had a maximum transmission of 100%. For the wide filters, we used βwide100g represented by the red circles, βwide125g represented by the green circles, βwide150g represented by the blue circles, βwide175g represented by

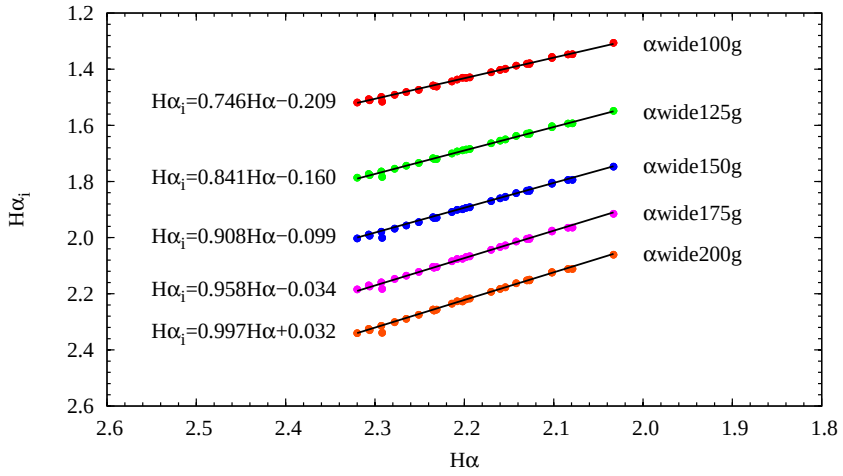

Figure 3.5 Instrumental Hα vs Standard Hα. These measurements were made using the filter αnarrow30g in combination with five wide filters. Each wide filter is listed to the right of each data set. The equation of the line of best fit is listed to the left of each data set.

the purple circles, and βwide200g represented by the orange circles. All five sets of data had R^2 values greater than 0.99 and the slope for each data set has a standard error of less than 0.005. The filter combination with the greatest slope is the narrow Hβ filter, which has a FWHM of 28 Å, and the wide filter with a FWHM of 200 Å. The current standard Hβ filters have FWHM of 30 Å and 130 Å. It is possible to get better sensitivity if we were to use a wide filter with 200 Å, but the Hβ filters have been standardized for such a long time that it would not be productive to suggest a new set of standard Hβ filters.

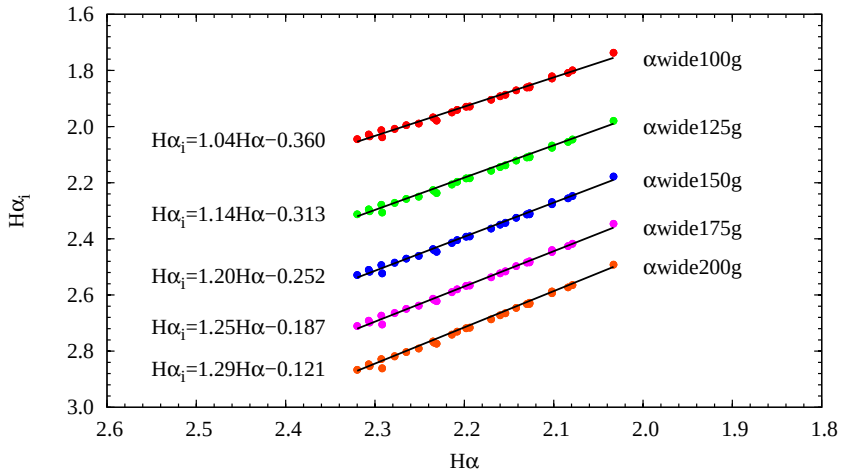

Figure 3.6 Instrumental Hα vs Standard Hα. These measurements were made using the filter αnarrow20g in combination with five wide filters. Each wide filter is listed to the right of each data set. The equation of the line of best fit is listed to the left of each data set.

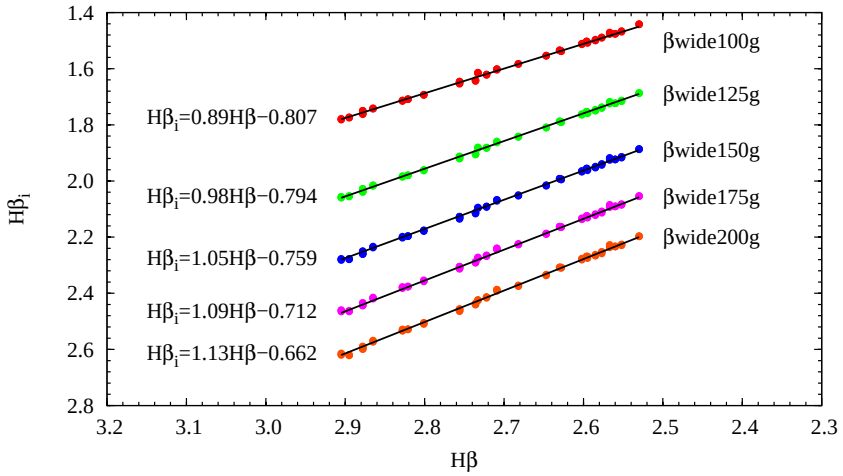

Figure 3.7 Instrumental Hβ vs Hβ. These measurements were made using the standard Hβ narrow filter scaled to a transmission of 100% in combination with five wide filters. Each wide filter is listed to the right of each data set. The equation of the line of best fit is listed to the left of each data set.

Chapter 4

Conclusions

We wanted to confirm that the Hα absorption line can be used to create a temperature index. The Hβ absorption line has already been shown to be a strong indicator of temperature and we expected the Hα absorption line to be an equal if not a stronger indicator of temperature. Our analysis indicates that the Hα index has a very strong correlation to the Hβ index with a relation of Hα=0.633Hβ+0.487 which has an R^2 value of 0.985.

We compared the Hα and Hβ indices to the b-y color index and to temperature. The results that we saw were expected and we were able to find a strong correlation between both Hα and Hβ indices. The Hα vs. Temperature relation that we found was Hα=7.20*10^{-5}T+1.72 with an R^2 value of 0.987. The Hβ vs. Temperature relation that we found was Hβ=1.11*10^{-4}T+1.95 with an R^2 value of 0.98.

We also tested several combinations of theoretical narrow and wide filters to see if we could obtain better sensitivity with filters that have different FWHM values. We found that for the Hα index, using a filter combination with a narrow filter with a FWHM of 20 Å and a wide filter with a FWHM of 200 Å is best for creating a temperature index.

Future Research

The Hα absorption line is stronger in cooler stars than the Hβ line and therefore the Hα index should be a better temperature indicator than the Hβ index. More data needs to be obtained on cooler stars so we can make a more definitive comparison between the Hα and Hβ indices.

Bibliography

Adams, L. 2009, Senior Thesis, Brigham Young University

Carroll, B. W. & Ostlie, D. A. 1996, "An Introduction to Modern Astrophysics" (Addison-Wesley Publishing Company, Inc.)

Crawford, D. L., Barnes, J. V., Faure, B. Q., Golson J. C. & Perry, C. L. 1966, AJ, 71:709

Crawford, D. L., Barnes, J. V., Gibson, J., Golson J. C. & Perry, C. L., Crawford M. L. 1972, A&AS, 5:109

Crawford, D. L., Mander, J. 1966, AJ, 71:114

Crawford, D. L., Perry, C. L. 1966, AJ, 71:206

Hauck, B. & Mermilliod, M. 1980, A&AS, 40:1

Laverty, C. L. 2006, Senior Thesis, Brigham Young University

SIMBAD database 2010, (http://simbak.cfa.harvard.edu/simbad/)

Taylor, B. J. & Joner, M. D., 1992, PASP, 104:911

Zeilik, M. & Gregory, S. A. 1998, "Introductory Astronomy & Astrophysics" (Saunders College Publishing)

Appendix A

Sources for Temperature Values

Since temperature values play an integral role in this project, we felt it necessary to cite all of the sources of temperature values we used. Table A.1 shows the sources for the temperature values in Table 2.1. The star names and their corresponding temperatures ar also listed. All of the temperature values for the Hyades cluster came from a single source but all other values came from several different sources.

Table A.1. Sources of Temperature Values in Table 2.1

Star	Temperature K	Source
HR 63	8960	1995A&A...294..536H
HR 675	9260	1993A&A...276..142H
HR 458	6140	2000AJ....119..390G
HR 493	5201	1990ApJS...74.1075M
vB 6	6876	2005ApJS...159..100T
vB 10	5922	2005ApJS...159..100T
vB 13	6528	2005ApJS...159..100T
vB 19	6230	2005ApJS...159..100T
vB 33	7534	2005ApJS...159..100T
vB 35	6462	2005ApJS...159..100T
vB 37	6580	2005ApJS...159..100T
vB 44	6380	2005ApJS...159..100T
vB 48	6146	2005ApJS...159..100T
vB 47	8025	2005ApJS...159..100T
vB 53	6747	2005ApJS...159..100T
vB 54	8208	2005ApJS...159..100T
vB 55	7315	2005ApJS...159..100T
vB 56	9231	2005ApJS...159..100T
vB 74	7683	2005ApJS...159..100T
vB 84	7294	2005ApJS...159..100T
vB 108	7987	2005ApJS...159..100T
vB 129	8038	2005ApJS...159..100T
HR 2880	7636	1990A&A...227..156B
HR 3951	5753	2008A&A...480...91S
HR 4540	6100	1998A&A...338..623M
Tr 62	8129	1987ApJ...321..967B
Tr 90	6380	1992ApJ...387..170F
Tr 145	7875	1987ApJ...321..967B
Tr 162	6345	1992ApJ...387..170F
Tr 183	8400	1987ApJ...321..967B
HR 5011	5866	2000A&AS..141..491C

Table A.1 (continued)

Star	Temperature K	Source
HR 5270	4500	2000ApJ...530..783W
HR 5447	6700	2000ApJ...530..939C
HD 140283	5650	2000AJ....120.1841F
HR 5933	6254	1998A&A...338..161F
HR 5936	6908	1990ApJ...354..310B
HR 5968	5782	1993A&A...275..101E
HD 161817	7636	2007MNRAS.374..664C
HR 7069	8542	1969PTarO..38..115L
HR 7178	10080	1986MNRAS.219..479B
HR 7462	5298	2008A&A...480...91S
HR 7469	6700	2000ApJ...530..939C
HR 7503	5800	2000A&A...364..249M
HR 7504	5760	2000AJ....119.2437D
HR 7534	6289	1996A&A...314..191G
HR 7560	6090	2000A&A...364..249M
HR 7610	9509	1989A&A...225..125L
HR 7977	14900	2007MNRAS.374..664C
HR 8279	17760	2007MNRAS.374..664C
HR 8969	6170	2007MNRAS.374..664C
HR 9088	5413	2008A&A...480...91S